Chapter 4

Effect of Overlapping Fe/TiO_2 Coated on Netlike Glass Disc and Cu Disc on CO_2 Reduction

Akira Nishimura

Additional information is available at the end of the chapter

http://dx.doi.org/10.5772/intechopen.70389

Abstract

Fe-doped TiO_2 (Fe/TiO_2) film photocatalyst was prepared by sol-gel and dip-coating process to respond to the visible spectrum. Netlike glass fiber and Cu disc that are base materials used for coating Fe/TiO_2 were investigated to promote the CO_2 reduction performance of the photocatalyst. The prepared Fe/TiO_2 film coated on netlike glass fiber and Cu disc was characterized by scanning electron microscope (SEM) and electron probe micro analyzer (EPMA). Additionally, the CO_2 reduction experiment using Fe/TiO_2 film coated on netlike glass disc, Cu disc, and their overlap was carried out by illuminating an Xe lamp or without ultraviolet (UV) light, respectively. As a result, the concentration of produced CO increases by Fe doping irrespective of base material used under the illumination condition with UV light as well as without UV light. The peak concentration of CO for the Fe/TiO_2 double overlapping is approximately 1.5 times as large as the Fe/TiO_2 single overlapping under the illumination condition with UV light due to the promotion of electron transfer between the two overlapped photocatalysts. However, the promotion ratio is approximately 1.1 times under the illumination condition without UV light.

Keywords: photocatalyst, Fe-doped TiO_2, CO_2 reduction, base material, overlapping effect

1. Introduction

After the industrial revolution, the averaged concentration of CO_2, which causes the global warming in the world, has been increased from 278 to 400 ppmV by 2015 [1]. Therefore, it requested a new CO_2 reduction or utilization technology in order to recycle CO_2.

According to the review of CO_2 conversion technologies [2], there are six vital CO_2 conversions: chemical conversions, electrochemical reductions, biological conversions, reforming,

inorganic conversions, and photochemical reductions [3]. Recently, artificial photosynthesis or the photochemical reduction of CO_2 to fuel has become an attractive route due to its economically and environmentally friendly behavior [2].

TiO_2 is the principal catalyst for almost all types of photocatalytic reaction. It is well known that CO_2 can be reduced into fuels such as CO, CH_4, CH_3OH and H_2, and so forth by using TiO_2 as the photocatalyst under ultraviolet (UV) light illumination [4–9]. After practical application of this technology, a carbon circulation system would then be established: CO_2 from the combustion of fuel produced by TiO_2 is reformed to fuels again using solar energy, and true zero emission can be achieved. However, the CO_2 reduction performance of TiO_2 is still low. One of the barriers to realize a carbon circulation system utilizing solar energy is that TiO_2 is only photoactive at the wavelength below 400 nm due to its relatively large band gap energy (~3.2 eV) [10].

Recently, studies on CO_2 photochemical reduction by TiO_2 have been carried out from the viewpoint of performance promotion by extending absorption range toward visible region [11–15]. Noble metal doping such as Pt, Pd, Rh, Au and Ag [11], nanocomposite CdS/TiO_2 combining two different band gap photocatalysts [12], N_2-modified TiO_2 [13], light harvesting complex of green plant–assisted Rh-doped TiO_2 [14] and dye-sensitized TiO_2 [15] have been developed for this process. However, the concentration in the products achieved is still low, ranging from 10 to 1000 ppmV [4, 6–9] or from 1 to 100 μmol/g-cat [11–15]. Therefore, the big breakthrough for increasing the concentration level of products is necessary to advance the CO_2 reduction technology in order to make the technology practically useful.

In the present paper, TiO_2 sol-gel and dip-coating process with doping is adopted in order to extend its photoresponsivity to the visible spectrum to promote the CO_2 reduction performance. This process can incorporate dopants into TiO_2 lattice, resulting in better optical and catalytic properties [16]. In addition, the integration of dopants into the sol during the gelation process facilitates direct interaction between TiO_2 and dopants during the sol-gel process [17].

It was reported that doping transition metal was a useful technique for extending the absorbance of TiO_2 into the visible region [18]. For doping, various metal ions have been used, but among them, Fe^{3+} is considered as a strong candidate as it has a similar radius to Ti^{4+} (Fe^{3+} = 78.5 pm, Ti^{4+} = 74.5 pm) [19] and can easily fit into the crystal lattice of TiO_2 [18, 20, 21]. Moreover, the redox potential (energy differential) of Fe^{2+}/Fe^{3+} is close to that of Ti^{3+}/Ti^{4+}, resulting in shifting its optical absorption into the visible region [18, 20, 21]. Due to easy availability as well as the above-described characteristics, Fe is selected as the dopant in the present study.

In the present study, a net glass fiber (SILIGLASS U, produced by Nihonmuki Co.) and Cu disc are used as base materials for coating TiO_2 film by sol-gel and dip-coating process. **Figure 1** shows the netlike glass disc, Cu disc, and two overlapped base materials. The netlike glass fiber is a net composed of glass fiber whose diameter is about 10 μm. The fine glass fibers are knitted, resulting in the diameter of aggregate fiber about 1 mm. According to the manufacture specifications of netlike glass fiber, the porous diameter of glass fiber is about 1 nm and the specific surface is about 400 m^2/g. The netlike glass fiber consists of SiO_2 whose purity is over 96 wt%. The aperture of net is about 2 × 2 mm. Since the netlike glass fiber has a porous characteristic, it is believed

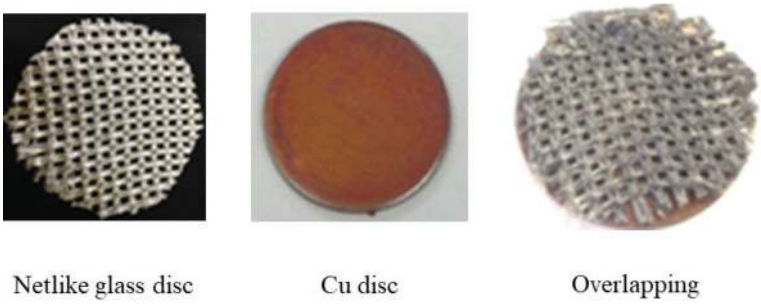

Figure 1. The base materials used for coating TiO_2 film.

that TiO_2 film and doped metal are captured by netlike glass fiber easily during sol-gel and dip-coating process. In addition, it can be expected that a CO_2 absorption performance of prepared photocatalyst is promoted due to the porous structure of netlike glass fiber. On the other hand, Cu disc is also adopted since the recombination of electron and hole produced by photochemical reaction can be prevented by a free electron emitted from Cu disc. The coupling effect of prepared photocatalysts coated on overlapped netlike glass fiber and Cu disc on CO_2 reduction performance is investigated. The illumination light is able to penetrate through the netlike glass fiber and reach on Cu disc. If the synergy effect between the photocatalyst coated on netlike glass fiber and that on Cu disc was obtained due to an active electron transfer between them, the promotion of CO_2 reduction performance would be achieved. There is no previous study on the coupling effect on CO_2 reduction performance of metal-doped TiO_2 or nondoped TiO_2.

In the present study, TiO_2 film doped with Fe (Fe/TiO_2) was prepared and characterized by scanning electron microscope (SEM) and electron probe micro analyzer (EPMA) analysis. The CO_2 reduction characteristics of Fe/TiO_2 coated on netlike glass fiber and/or Cu disc under the condition of illuminating Xe lamp with or without UV light were investigated.

2. Experimental

2.1. Procedure to prepare Fe/TiO_2 film

Sol-gel and dip-coating process, which is a general procedure, was selected to prepare Fe/TiO_2 film. TiO_2 sol solution consists of $[(CH_3)_2CHO_4]$ Ti (purity of 95 wt%, produced by Nacalai Tesque Co.) of 0.3 mol, anhydrous C_2H_5OH (purity of 99.5 wt%, produced by Nacalai Tesque Co.) of 2.4 mol, distilled water of 0.3 mol and HCl (purity of 35 wt%, produced by Nacalai Tesque Co.) of 0.07 mol. Fe particles (produced by Merck KGaA, particle size below 10 μm) were added to TiO_2 sol solution. Netlike glass fiber was cut to disc, and its diameter and thickness were 50 and 1 mm, respectively. The Cu disc used has diameter and thickness of 50 and 1 mm, respectively. The base material was dipped into Fe/TiO_2 sol solution at the speed of 1.5 mm/s and pulled up at the fixed speed of 0.22 mm/s. Then, it was dried out and fired under the controlled firing temperature (FT) and firing duration time (FD), with Fe/TiO_2 film

fastened on the base material. FT and FD were set at 623 K and 180 s, respectively. The ratio of amount of added Fe to amount of TiO_2 sol solution (R) was set at 10 wt%.

2.2. Characterization of Fe/TiO_2 film

The surface structure and crystallization characteristics of Fe/TiO_2 film were evaluated by SEM (JXA-8530F, produced by JEOL Ltd.) and EPMA (JXA-8530F, produced by JEOL Ltd.). Since these two measuring instruments use electron for analysis, the sample should be an electron conductor. Though Cu disc is a good electron conductor, netlike glass disc is not an electron conductor. In this study, the carbon vapor deposition was conducted by the dedicated device (JEE-420, produced by JEOL Lt.) for Fe/TiO_2 coated on netlike glass disc before analysis by SEM and EPMA. The thickness of carbon deposited on sample was approximately 20–30 nm. The electron probe emits the electron to the sample under an acceleration voltage of 15 kV and a current of 3.0×10^{-8} A; the surface structure of sample is analyzed by SEM. The characteristics of X-ray are detected by EPMA at the same time, resulting in the concentration of chemical element analyzed according to the relationship between the characteristics of X-ray energy and the atomic number. The spatial resolution of SEM and EPMA is 10 μm. The EPMA analysis helps not only to understand the coating state of prepared photocatalyst but also to measure the amount of doped metal within TiO_2 film on the base material.

2.3. CO_2 reduction experiment

Figure 2 shows that experimental setup of the reactor consisting of stainless pipe (100 mm (H) × 50 mm (ID)), a netlike glass or Cu that is disc shaped (50 mm (D) × 1 mm (t)) with Fe/TiO_2 film placed on the Teflon cylinder (50 mm (H) × 50 mm (D)), a quartz glass disc (84 mm

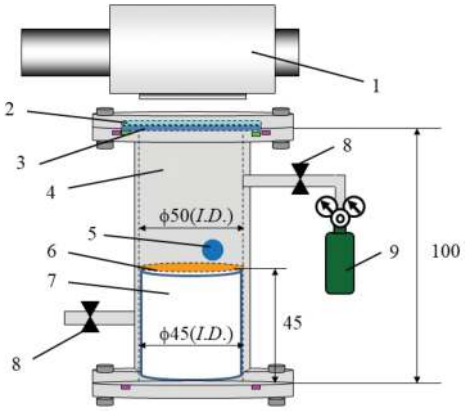

1. Xe lamp, 2. Sharp cut filter, 3. Quartz glass disc, 4. Stainless pipe,
5. Gas sampling tap, 6. Photocatalyst, 7. Teflon cylinder, 8. Valve,
9. CO_2 gas cylinder (99.995 vol%)

Figure 2. Schematic drawing of CO_2 reduction experimental setup.

(D) × 10 mm (t)), a sharp cut filter cutting off the light whose wavelength is below 400 nm (SCF-49.5C-42 L, produced by SIGMA KOKI Co. Ltd.), Xe lamp (L2175, produced by Hamamatsu Photonics K. K.) and CO_2 gas cylinder (purity of 99.995 vol%).

The size of reactor for charging CO_2 is 1.25×10^{-4} m^3. The Xe lamp illuminates the netlike glass disc or Cu disc coated with Fe/TiO_2 film, which is located inside the stainless pipe, through the sharp cut filter and the quartz glass disc that are at the top of the stainless pipe. The Xe lamp illuminates the light whose wavelength ranged from 185 to 2000 nm. A sharp cut filter can remove UV components of the light, resulting in the wavelength of light from Xe lamp ranging from 401 to 2000 nm. **Figure 3** indicates that the sharp cut filter can remove the light whose wavelength ranged below 400 nm. During the experiment, the light intensity of Xe lamp illuminating the photocatalyst without and with setting the sharp cut filter is estimated at 81.9 and 60.7 mW/cm^2, respectively.

To start CO_2 reduction experiment in this study, CO_2 gas whose purity was 99.995 vol% was flowed through the reactor as a purged gas for approximately 15 min. The valves at the inlet and the outlet of reactor were closed after charging CO_2. The gas pressure and gas temperature in the reactor were set at 0.1 MPa and 298 K, respectively, the distilled water of 100 μL was injected into the reactor through a gas pipe and Xe lamp was started to illuminate at the same time. The water injected vaporized completely in the reactor. Since Xe lamp emits the heat, the gas temperature in reactor was attained at 343 K within an hour and maintained at approximately 343 K during the experiment. The water of 5.56 mmol and CO_2 of 576 mmol were in the reactor. The gas in the reactor was sampled by a gas syringe every 24 h during the experiment, which was analyzed by FID gas chromatograph (GC353B, produced by GL Science) and methanizer (MT221, produced by GL Science). FID gas chromatograph and methanizer can detect a gas whose concentration is 1 ppmV order level.

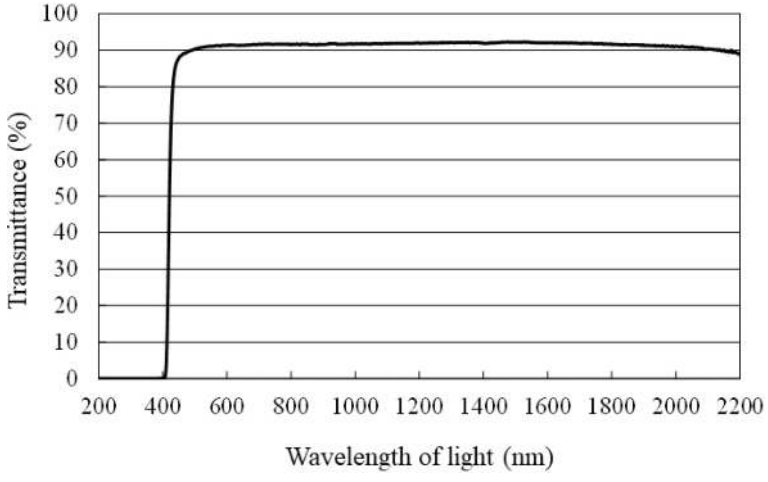

Figure 3. Light transmittance data of sharp cut filter.

3. Results and discussion

3.1. Characterization of Fe/TiO_2 film by SEM and EPMA

Figures 4 and **5** show SEM images of TiO_2 and Fe/TiO_2 film coated on netlike glass disc, respectively. The SEM images were taken at 1500 times magnification under the acceleration voltage of 15 kV and the current of 3.0×10^{-8} A.

Figures 6 and **7** show EPMA images of TiO_2 and Fe/TiO_2 film coated on netlike glass disc, respectively. The EPMA analysis was carried out to obtain 1500 times magnified SEM images as shown in **Figures 4** and **5**. In EPMA image, the concentrations of each element in observation area are indicated by different colors. Dilute colors indicate that the amount of element is large, while dense colors indicate that the amount of element is small.

To identify the position of each element, the colored circles are added to these SEM and EPMA images. The red circles shown in SEM images of **Figures 4** and **5** indicate that the amount of Ti is large as pointed out in EPMA images of **Figures 6** and **7**. From these figures, it can be observed that TiO_2 film with teethlike shape is coated on netlike glass fiber. It is also seen that TiO_2 film builds a bridge among several glass fibers. It is believed that the temperature profile of TiO_2 solution adhered on the netlike glass disc is not uniform because the thermal conductivities of Ti and SiO_2 are different during firing process. The thermal conductivities of Ti and SiO_2 at 600 K are 19.4 and 1.82 W/(mK), respectively [22]. Since the thermal expansion and shrinkage around netlike glass fiber occur, thermal crack of TiO_2 film is caused. Therefore, TiO_2 film on netlike glass fiber is teethlike.

The yellow circle shown in SEM image of **Figure 5** indicates the existence of metal particles as pointed out in EPMA images of **Figure 7**. It is observed from **Figure 5** that Fe particles adhere on the netlike glass fiber directly. According to **Figure 5**, the size of doped metal is below

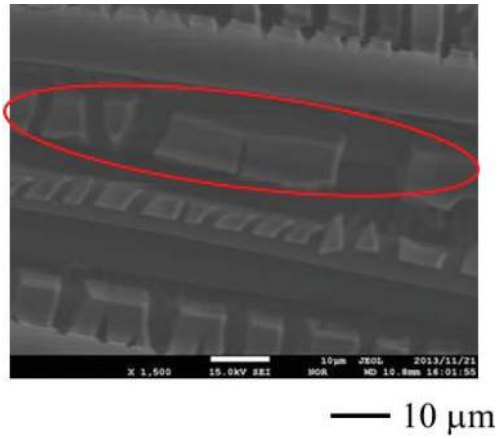

Figure 4. The SEM image of TiO_2 film coated on netlike glass disc.

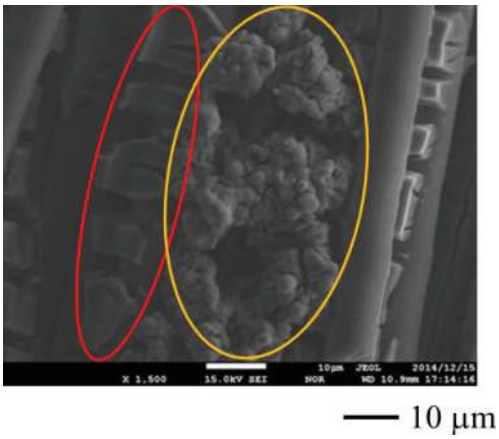

Figure 5. The SEM image of Fe/TiO_2 film coated on netlike glass disc.

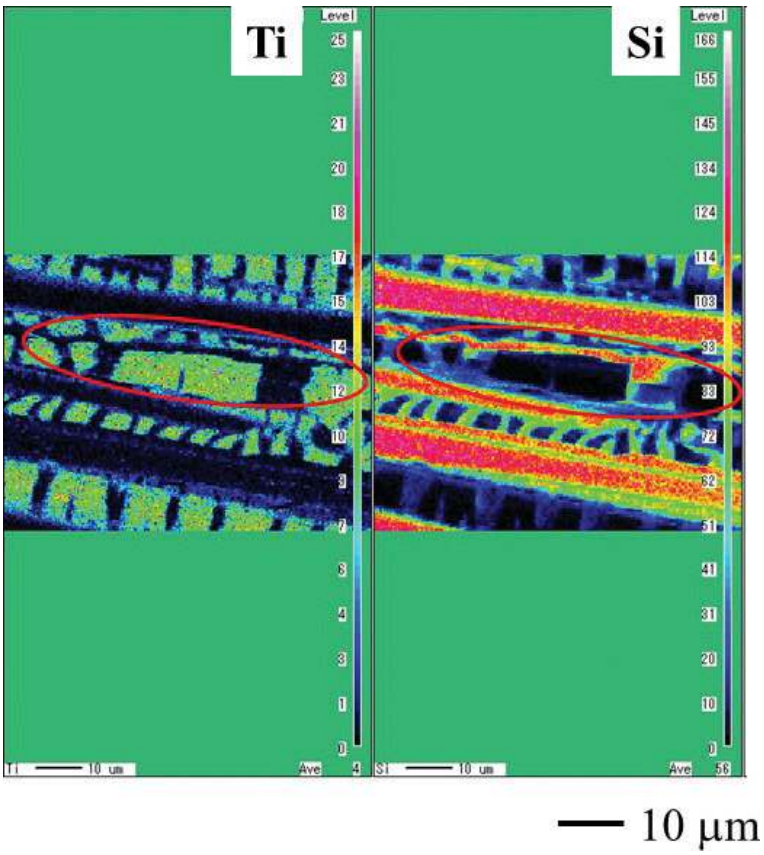

Figure 6. The EPMA image of TiO_2 film coated on netlike glass disc.

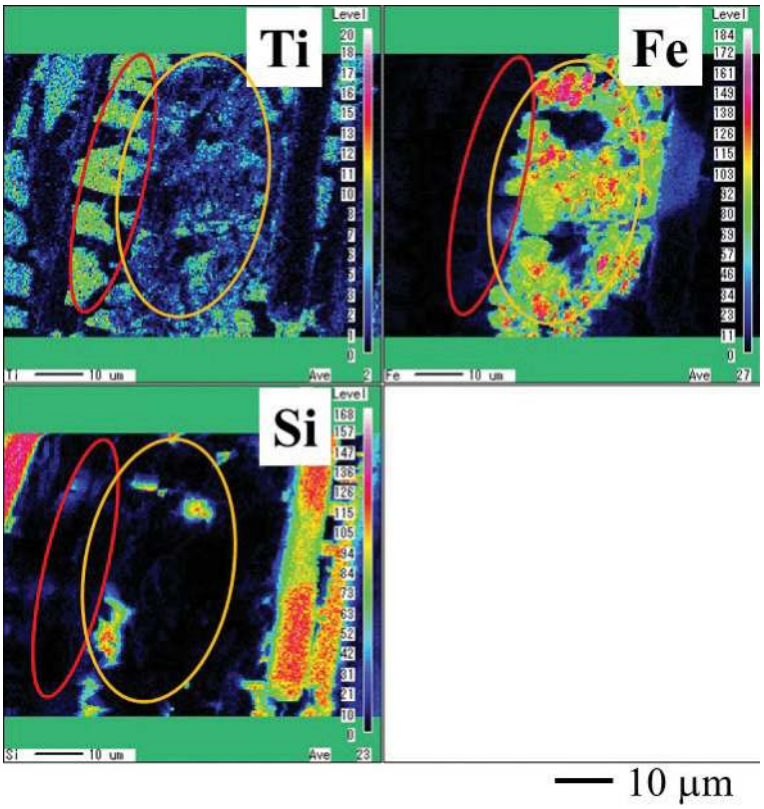

Figure 7. The EPMA image of Fe/TiO_2 film coated on netlike glass disc.

10 μm. Since the Fe particles used have diameters below 10 μm, it is confirmed that the Fe particles can be loaded without agglomeration by the sol-gel and dip-coating process.

Figures 8 and **9** show SEM image of TiO_2 and Fe/TiO_2 film coated on Cu disc, respectively. The SEM images were taken at 1500 times magnification under an acceleration voltage of 15 kV and a current of 3.0×10^{-8} A.

Figures 10 and **11** show EPMA images of TiO_2 and Fe/TiO_2 film coated on Cu disc, respectively. EPMA analysis was carried out to obtain 1500 times magnified SEM images as shown in **Figures 8** and **9**.

According to **Figures 9** and **11**, the TiO_2 film is contracted around Fe particles. The surface characteristics of TiO_2 or Fe/TiO_2 are explained as follows [23]:

i. Before firing process, TiO_2 or Fe/TiO_2 sol solution is adhered on Cu disc uniformly.

ii. The temperature profile of TiO_2 or Fe/TiO_2 sol solution adhered on Cu disc is not uniform during firing process since the thermal conductivities of Cu, Ti and Fe are different. Thermal conductivities of Cu, Ti and Fe at 600 K are 383, 19.4, and 54.7 W/(mK),

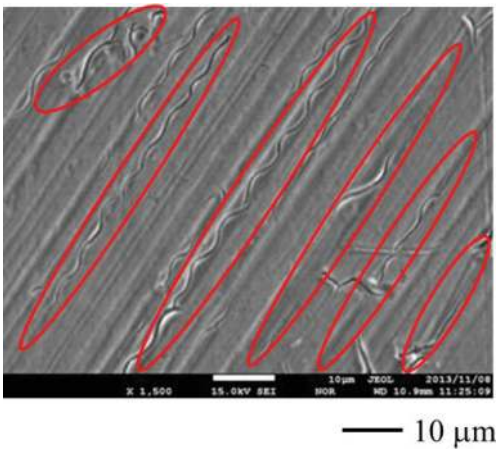

Figure 8. SEM image of TiO_2 film coated on Cu disc.

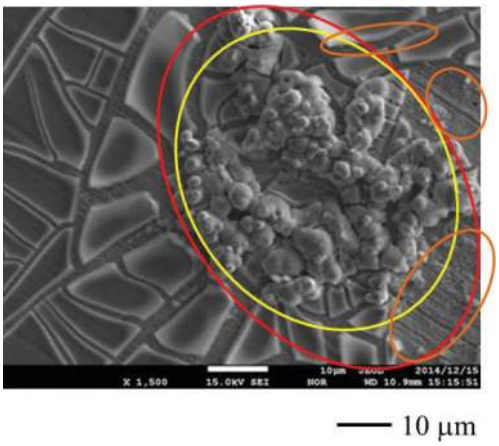

Figure 9. SEM image of Fe/TiO_2 film coated on Cu disc.

respectively [22]. Therefore, the thermal expansion around Fe particles and the thermal shrinkage around the other areas of TiO_2 sol occur for Fe/TiO_2, while the thermal expansion and shrinkage between TiO_2 and Cu disc occur for nonmetal-doped TiO_2 film.

iii. Because of thermal stress caused by the uneven distribution of temperature, the cracks around Fe and the shrinkage of TiO_2 film around the cracks occur after firing process. Therefore, a large amount of Cu pointed out by orange circles, which is an element of basis Cu disc, around Fe is observed in **Figure 11**. In addition, a large amount of Ti around Fe is also seen in the same figure.

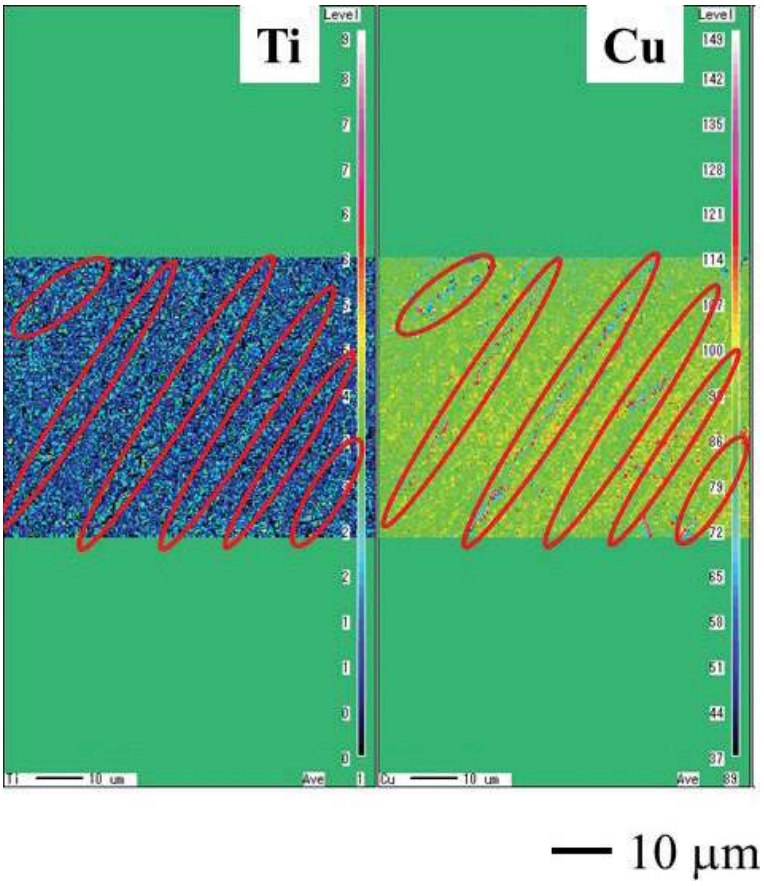

Figure 10. EPMA image of TiO_2 film coated on Cu disc.

The center of netlike glass disc or Cu disc whose diameter is 300 μm is analyzed by EPMA to evaluate the amount of doped Fe within TiO_2 film quantitatively. The ratio of Fe to Ti is measured by averaging the data detected by EPMA.

Table 1 lists weight percentages of elements Fe and Ti in the Fe/TiO_2 film coated on netlike glass disc or Cu disc. From this table, it can be seen that more Fe is contained in the Fe/TiO_2 film on netlike glass disc than that on Cu disc, under the doping condition, that is, R of 10 wt%. As expected, the netlike glass fiber can capture the dopant metal powder well during dip-coating process due to the porous structure. However, Cu disc hardly captures the dopant metal powder during dip-coating process since the surface of Cu disc is smooth. From these results, it is clear that the amount of dopants that could be doped is influenced by the base material when the sol-gel and dip-coating process is adopted for metal doping.

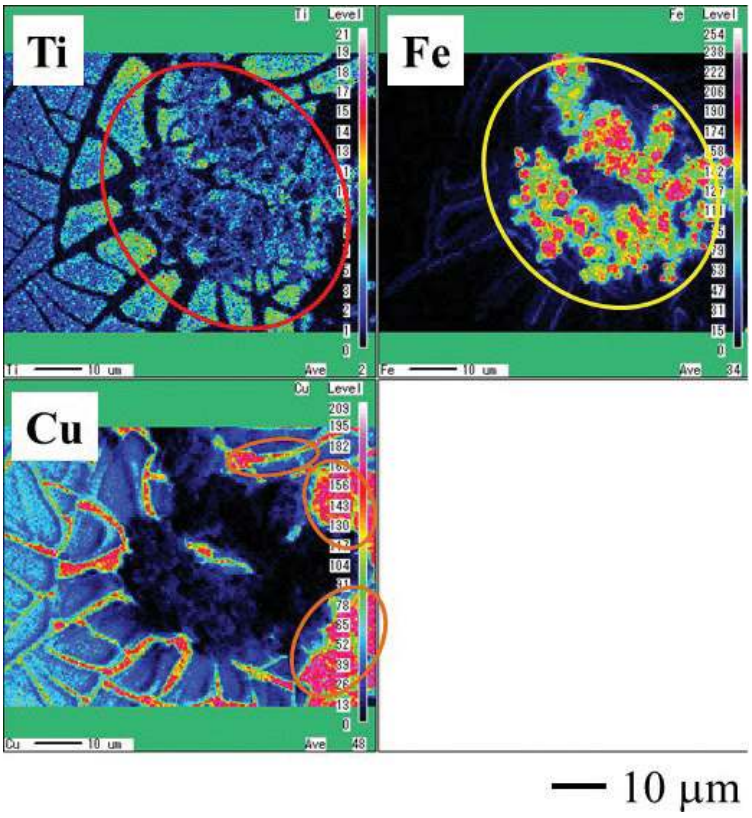

Figure 11. EPMA image of Fe/TiO_2 film coated on Cu disc.

Photocatalyst type	Weight ratio		
	Ti (wt%)	Fe (wt%)	Total (wt%)
Fe/TiO coated on netlike glass disc	74.76	25.24	100
Fe/TiO coated on Cu disc	98.15	1.85	100

Table 1. Weight ratio of elements Fe and Ti within the prepared metal-doped TiO_2 film.

3.2. CO_2 reduction characteristics of Fe/TiO_2 coated on netlike glass disc or Cu disc

Figure 12 shows the concentration changes of CO produced in the reactor along the time under the Xe lamp with UV light on, for TiO_2 or Fe/TiO_2 film coated on netlike glass disc or Cu disc or their overlap. In this figure, a single overlapping means the photocatalyst coated on the upper surface of netlike glass disc is overlapped over the photocatalyst coated on Cu disc, while a double overlapping means that the photocatalyst coated on both the upper and lower surfaces of netlike glass disc is overlapped over the photocatalyst coated on Cu disc. In

this experiment, CO is the only fuel produced from the reactions. The reaction scheme for CO production by the photochemical reaction with CO_2 and H_2O is shown as follows [4, 7, 24–26]:

$$TiO_2 + hv \rightarrow h^+ + e^- \quad (1)$$

$$H_2O + h^+ \rightarrow \cdot OH + H^+ \quad (2)$$

$$\cdot OH + H_2O + h^+ \rightarrow O_2 + 3H^+ \quad (3)$$

$$CO_2 + 2H^+ + 2e^- \rightarrow CO + H_2O \quad (4)$$

In the first step, hole h^+ and electron e^- are generated by illuminating light on photocatalyst as shown in Eq. (1). The generated hole reacts with H_2O in the oxidation reaction step, resulting in proton H^+ produced as shown in Eqs. (2) and (3). The proton and electron react with CO_2 in the reduction reaction step, resulting that CO is produced as shown in Eq. (4).

Since the concentrations of CO in most experiments started to decrease after illumination of 48-72 hours for illumination conditions with UV light due to the reverse reaction by CO and O_2, which is a by-product as shown in Eq. (3). **Figure 12** shows only the concentration up to 72 h. Before the experiments, a blank test, which was running the same experiment without illumination of Xe lamp, had been carried out to set up a reference case. No fuel was produced in the blank test as expected.

According to **Figure 12**, the concentration of CO increases due to Fe doping irrespective of base material. The improvement of photocatalytic performance by Fe doping under the illumination condition with UV light can be caused by the generation of shallow charge traps in

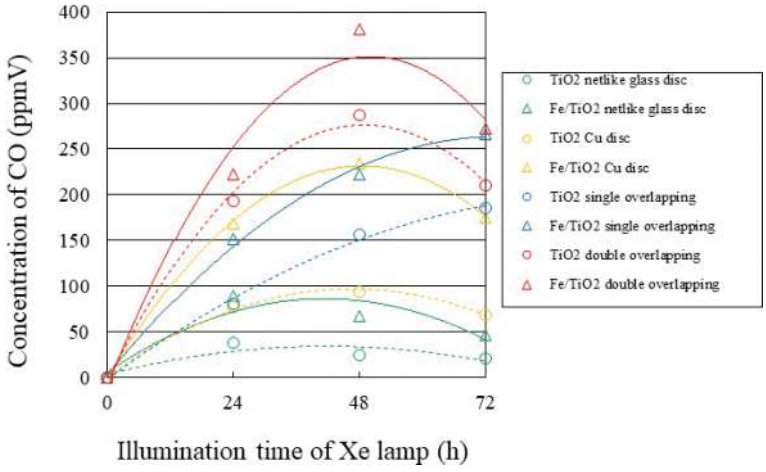

Figure 12. Comparison of concentrations of produced CO among photocatalysts coated on different base materials under the illumination condition with UV light.

the crystal structure, which decreases the recombination rate of electron-hole pairs [20]. In addition, the concentration of CO produced by Fe/TiO_2 coated on Cu disc is higher than that on netlike glass disc. Though the weight ratio of Fe for Fe/TiO_2 coated on netlike glass disc is larger than that on Cu disc as shown in **Table 1**, the reaction surface area, which can receive the light, is small due to aperture of net. Therefore, the photocatalytic performance of Fe/TiO_2 coated on netlike glass disc is lower than that on Cu disc. Moreover, the Fe/TiO_2 single overlapping shows the small superiority over Fe/TiO_2 coated on netlike glass disc and Fe/TiO_2 coated on Cu disc. Although the present study expected the positive synergy effect of combination of two photocatalysts coated on different base materials, the positive effect observed was very small. Since the netlike glass fiber consists of SiO_2, which is an electrical insulation material, the electron transfer between the two overlapped photocatalysts might not be realized well. However, in the experiment of Fe/TiO_2 double overlapping, the photocatalytic performance is promoted, resulting that the peak concentration of CO is approximately 1.5 times as large as the Fe/TiO_2 single overlapping. The reason is thought to be that the electron transfer between two overlapped photocatalysts is promoted, resulting that the synergy effect of combination of two photocatalysts coated on different base materials is obtained.

Figure 13 illustrates the difference of electron transfer phenomenon between single and double overlapping. In this figure, the hole produced by photochemical reaction is not shown mainly to clarify the electron transfer phenomenon. It is believed that the path for electron transfer is constructed by double overlapping.

Figure 14 shows the comparison of molar quantities of CO per weight of photocatalyst among the prepared photocatalysts. These values are estimated based on the maximum CO obtained under the illumination condition with UV light up to 72 h. According to this figure, the molar quantity of CO per weight of Fe/TiO_2 coated on Cu disc shows the highest performance since the weight of Fe/TiO_2 coated on Cu disc (= 0.02 g-cat) is smaller than that on netlike glass disc (= 0.25 g-cat). Though the netlike glass fiber captures the large amount of TiO_2 sol and Fe particle during dipping process well, some Fe/TiO_2 adhered in the pores of netlike glass fiber might not be activated well due to the lack of light illumination. Although it is believed that

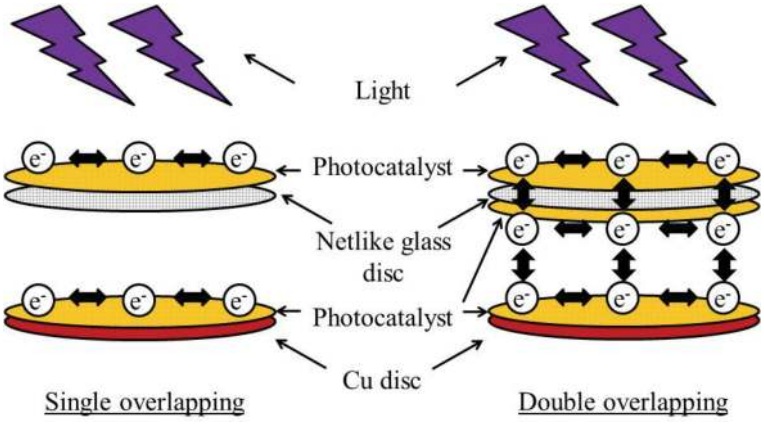

Figure 13. Comparison of electron transfer phenomena between single and double overlapping.

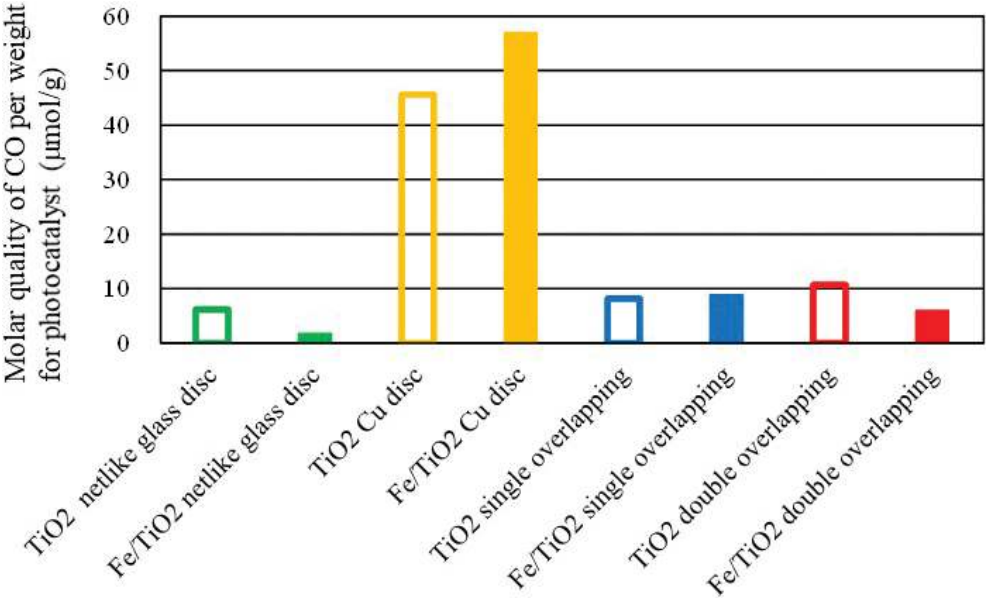

Figure 14. Comparison of CO_2 reduction performances per weight of photocatalyst under the illumination condition with UV light.

the Fe doping could assist CO_2 reduction if the light could illuminate inside the pore of netlike glass disc, the positive effect of Fe doping on CO_2 reduction performance per weight of photocatalyst base under the overlapping condition was not as significant as that in the case of Fe/TiO_2 coated on netlike glass disc. In addition, the mass transfer in the space between the two photocatalysts coated on netlike glass disc and Cu disc should be enhanced in order to meet the photoreaction rate under the overlapping condition. If the produced fuel remains in the space between two photocatalysts, the reactant of CO_2 and H_2O could be blocked to reach the surface of photocatalyst, resulting that the photochemical reaction could not be carried out well even though the light is illuminated for the photocatalyst. Therefore, it is necessary to control the amount of doped Fe, which is coated on the surface and on the pore of the netlike glass fiber, as well as to optimize the aperture of netlike glass fiber.

Figure 15 shows the concentration changes of CO produced in the reactor along the time under the Xe lamp illumination without UV light, for TiO_2 or Fe/TiO_2 film coated on netlike glass disc or Cu disc or their overlap. In this experiment, CO is the only fuel produced from the reactions. Since the concentration of CO almost started to decrease after illumination of 72–96 h for all cases due to the reverse reaction by CO and O_2, which is the by-product as shown in Eq. (3), **Figure 15** shows the concentration only up to 96 h.

From **Figure 15**, it can be seen that the CO_2 reduction performance of TiO_2 is promoted by Fe doping due to extension of the photoresponsivity of TiO_2 to the visible spectrum as well as decrease in the recombination rate of electron-hole pairs by the generation of

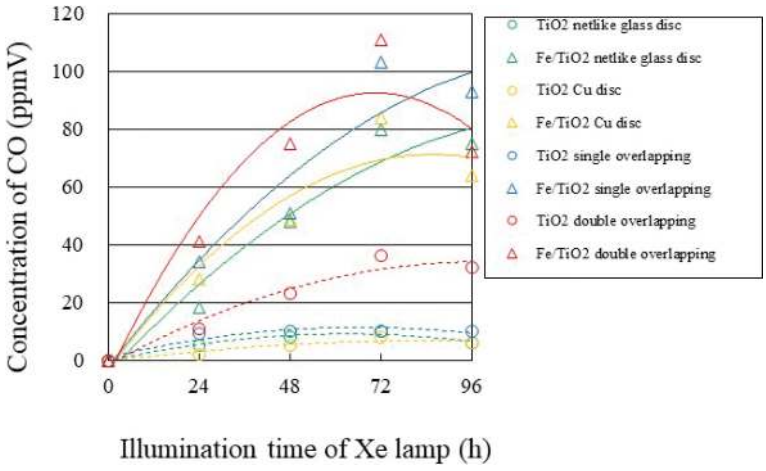

Figure 15. Comparison of concentrations of produced CO among the photocatalysts coated on different base materials under the illumination condition without UV light.

shallow charge traps in the crystal structure. In addition, the maximum concentration of CO obtained by Fe/TiO_2 coated on netlike glass disc is almost the same as that by Fe/TiO_2 coated on Cu disc, which has a different tendency from the results obtained under the UV illumination condition. Under the illumination condition without UV light, it is believed that the amount of doped Fe is important to absorb the visible light to perform the photocatalytic reaction. Since the amount of doped Fe for Fe/TiO_2 coated on netlike glass disc is much larger than that for Fe/TiO_2 coated on Cu disc as shown in **Table 1**, the CO_2 reduction performance of Fe/TiO_2 coated on netlike glass disc equals that on Cu disc, while that on netlike glass disc is lower than that on Cu disc under the illumination condition with UV light.

Furthermore, according to **Figure 15**, the positive effect of overlapping is obtained, especially under the double overlapping condition. As mentioned before, since the netlike glass fiber consists of SiO_2, which is an electrical insulation material, the electron transfer between the two overlapped photocatalysts might not be realized well. However, the photocatalytic performance is promoted up to approximately 1.1 times by double overlapping when the maximum concentrations of CO are compared between the single and the double overlapping condition. The electron transfer between the two overlapped photocatalysts is promoted by double overlapping. However, compared to the previous cases with UV illumination, the improvement effect by double overlapping is small. Since the wavelength of illuminating light penetrating through netlike glass disc becomes longer due to losing energy, the electron produced by the Fe/TiO_2 coated on Cu disc, which is positioned under the netlike glass disc, decreases. The range of wavelength of light illuminating after penetrating through netlike glass disc is narrower than that in the UV illumination condition cases. Therefore, the effect of electron transfer promotion between the two overlapped photocatalysts is small compared with that in the UV illumination cases.

Figure 16 shows the comparison of molar quantities of CO per weight of photocatalyst among the prepared photocatalysts. These values are estimated based on the maximum CO obtained under the no-UV illumination condition up to 96 h. It reveals that the molar quantity of CO per weight of Fe/TiO_2 under the double overlapping condition is the highest among all experimental conditions. In addition, it also reveals the positive effect of overlapping on CO_2 reduction performance in terms of molar quantity of CO per weight of photocatalyst is achieved in both single and double overlapping cases. It is believed that Fe/TiO_2 coated on Cu disc, which is positioned under the netlike glass disc, can utilize at least some of the light penetrating through the aperture of netlike glass disc for photochemical reactions, although the wavelength of the penetrating light becomes long.

The bigger synergy effect in terms of molar quantity of CO per weight of photocatalyst for two overlapped photocatalysts in no-UV cases is achieved when comparing with UV illumination cases. Since the photochemical reaction rate and the amount of produced fuel are small under the no-UV illumination condition compared to those under UV light, it would be beneficial to the mass transfer between produced fuel and reactant of CO_2 and H_2O on the surface of photocatalyst in no-UV cases. As a result, the mass transfer and photochemical reaction are carried out effectively in no-UV cases. Therefore, the molar quantity of CO per weight of photocatalyst for overlapping cases is large in no-UV cases. According to previous reports [27, 28], the mass transfer is an inhibition factor to promote the CO_2 reduction performance of

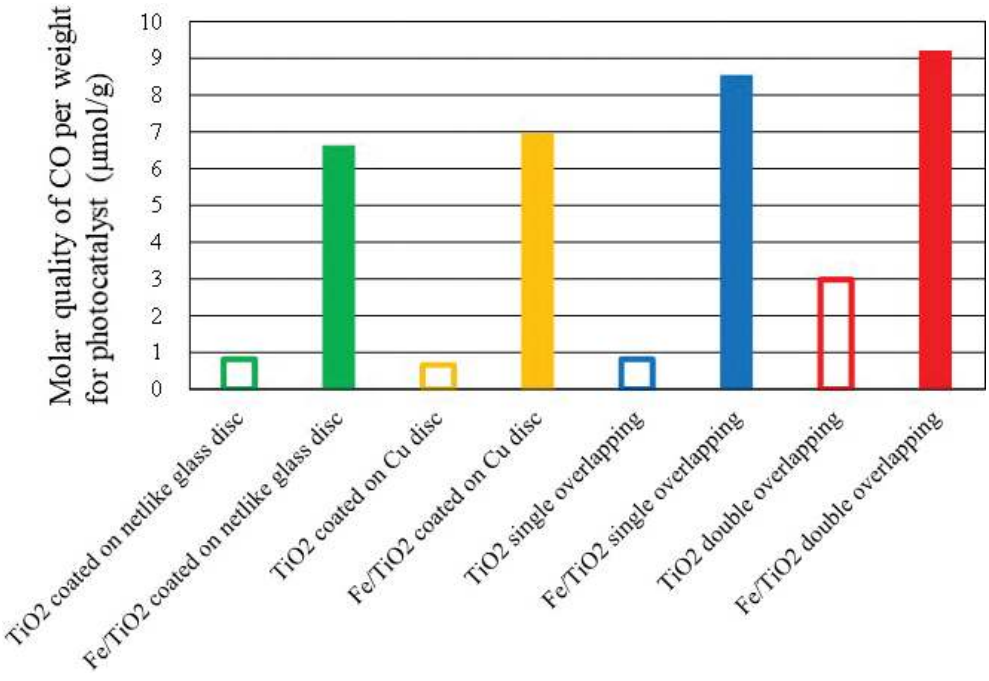

Figure 16. Comparison of CO_2 reduction performances per weight of photocatalyst under the illumination condition without UV light.

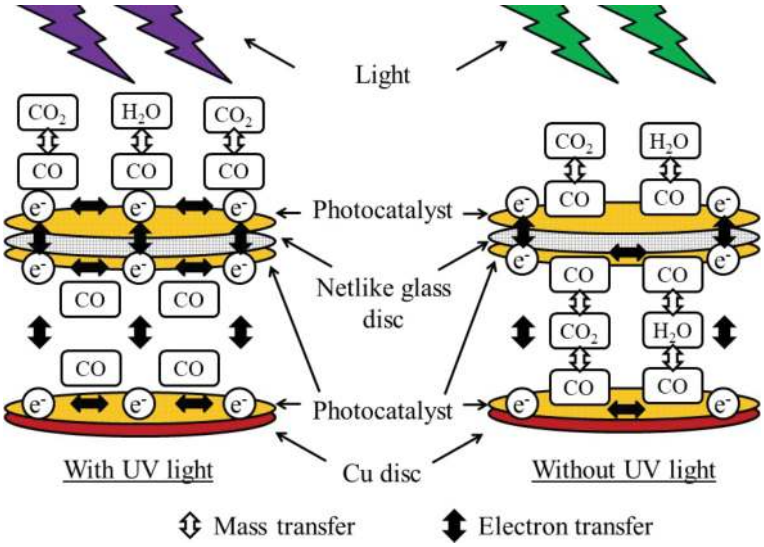

Figure 17. Comparison of mass and electron transfer within two overlapped photocatalysts between the illumination condition with UV light and that without UV light.

photocatalyst and it is necessary to control the mass transfer rate to meet the photochemical reaction rate. **Figure 17** illustrates the comparison of mass and electron transfer within two overlapped photocatalysts in UV and no-UV illumination cases.

Compared to the previous researches [4, 6–9, 11–15], the CO_2 reduction performance of photocatalysts prepared in the present study is almost at the same level. However, the present study clarifies that the double overlapping arrangement is effective in improving the CO_2 reduction performance of Fe/TiO_2. It, therefore, proposes that the netlike porous metal having an appropriate area of aperture can be a good base material for overlapping arrangement instead of netlike glass fiber since the former has a good electrical conductivity, light permeability, and gas diffusivity. In addition, the dopant like Cu, which can absorb the longer wavelength light than Fe [21], should be used in the layers at lower positioned photocatalysts in overlapping conditions. This proposal is similar to the concept of the hybrid photocatalyst using two photocatalysts having different band gaps [29–31].

4. Conclusions

Based on the investigation into this study, the following conclusions can be drawn:

1. TiO_2 film with teethlike shape could be coated on netlike glass fiber, and Fe fine particles are loaded without agglomeration. However, TiO_2 film would contract around Fe particles when Fe/TiO_2 was coated on the Cu disc.

2. The amount of dopants that could be coated is influenced by the base material used.
3. Under the UV illumination condition, the concentration of produced CO increases due to Fe doping irrespective of the base material used. The photocatalytic performance of Fe/TiO_2 coated on the netlike glass disc is lower than that on the Cu disc. The peak concentration of CO for the Fe/TiO_2 double overlapping is approximately 1.5 times as large as the Fe/TiO_2 single overlapping.
4. Under the illumination condition without UV light, the CO_2 reduction performance of TiO_2 is also promoted by Fe doping due to extension of the photoresponsibility of TiO_2 to the visible spectrum as well as decrease in the recombination rate of electron–hole pairs by the generation of shallow charge traps in the crystal structure. The positive effect of overlapping is obtained especially under the double overlapping condition. From the viewpoint of the molar quantity of CO per weight of photocatalyst, the Fe/TiO_2 double overlapping shows the highest performance. It is believed that the mass transfer rates between produced fuel and reactants on the surface of photocatalyst are better matched with the photochemical reaction rates when Fe/TiO_2 is double overlapped.
5. The double overlapping arrangement is effective for improving the CO_2 reduction performance of Fe/TiO_2.

Acknowledgements

The author would like to gratefully thank JSPS KAKENHI for grant no. 25420921, Tanikawa Foundation, and Mazda Foundation for the financial support for this work.

Author details

Akira Nishimura

Address all correspondence to: nisimura@mach.mie-u.ac.jp

Division of Mechanical Engineering, Graduate School of Engineering, Mie University, Tsu Mie, Japan

References

[1] The Japan Meteorological Agency. World Data Center for Greenhouse Gases [Internet]. 2001/07/02 [Updated: 2017/03/09]. Available from: http://ds.data.jma.go.jp/gmd/wdcgg/wdcgg.html [Accessed: 2017/06/08]

[2] Das S, Daud WMAW. Photocatalytic CO_2 transformation into fuel: A review on advances in photocatalyst and photoreactor. Renewable and Sustainable Energy Reviews. 2014;**39**:765-805

[3] Sakakura T, Choi J-C, Yasuda H. Transformation of carbon dioxide. Chemical Reviews. 2007;**107**:2365-2387

[4] Adachi K, Ohta K, Mizuno T. Photocatalytic reduction of carbon dioxide to hydrocarbon using copper-loaded titanium dioxide. Solar Energy. 1994;**53**:187-190

[5] Anpo M, Chiba K. Photocatalytic reduction of CO_2 on anchored titanium oxide catalysts. Journal of Molecular Catalysis. 1992;**74**:207-212

[6] Dey GR, Belapurkar AD, Kishore K. Photo-catalytic reduction of carbon dioxide to methane using TiO_2 as suspension in water. Journal of Photochemistry and Photobiology A: Chemistry. 2004;**163**:503-508

[7] Hirano K, Inoue K, Yatsu T. Photocatalysed reduction of CO_2 in aqueous TiO_2 suspension mixed with copper powder. Journal of Photochemistry and Photobiology A: Chemistry. 1992;**64**:255-258

[8] Ishitani O, Inoue C, Suzuki Y, Ibusuki T. Photocatalytic reduction of carbon dioxide to methane and acetic acid by an aqueous suspension of metal-doped TiO_2. Journal of Photochemistry and Photobiology A: Chemistry. 1993;**72**:269-271

[9] Kaneco S, Kurimoto H, Shimizu Y, Ohta K, Mizuno T. Photocatalytic reduction of CO_2 using TiO_2 powders in supercritical fluid CO_2. Energy. 1999;**24**:21-30

[10] Gui MM, Chai S-P, Xu B-Q, Mohamed AR. Enhanced visible light responsive MWCNT/TiO_2 core-shell nanocomposites as the potential photocatalyst for reduction of CO_2 into methane. Solar Energy Materials & Solar Cells. 2014;**122**:183-189

[11] Xie S, Wang Y, Zhang Q, Deng W, Wang Y. MgO and Pt-promoted TiO_2 as an efficient photocatalyst for the preferential reduction of carbon dioxide in the presence of water. ACS Catalysis. 2014;**4**:3644-3653

[12] Beigi AA, Fatemi S, Salehi Z. Synthesis of nanocomposite CdS/TiO_2 and investigation of its photocatalytic activity for CO_2 reduction to CO and CH_4 under visible light irradiation. Journal of CO_2 Utilization. 2014;**7**:23-29

[13] Michalkiewicz B, Majewska J, Kadziolka G, Bubacz K, Mozia S, Morawski AW. Reduction of CO_2 by adsorption and reaction on surface of TiO_2-nitorogen modified photocatalyst. Journal of CO_2 Utilization. 2014;**5**:47-52

[14] Lee C-W, Kourounioti RA, Wu JCS. Photocatalytic conversion of CO_2 to hydrocarbons by light-harvesting complex assisted Rh-doped TiO_2 photocatalyst. Journal of CO_2 Utilization. 2014;**5**:33-40

[15] Ozcan O, Yukruk F, Akkaya EU, Uner D. Dye sensitized CO_2 reduction over pure and platinized TiO_2. Topics in Catalysis. 2007;**44**:523-528

[16] Subramanian M, Vijayalakshmi S, Venkataraj S, Jayavel R. Effect of cobalt doping on the structural and optical properties of TiO_2 film prepared by sol-gel process. Thin Solid Films. 2008;**516**:3776-3782

[17] Zabova H, Cirkva V. Microwave photocatalysis III. Transition metal ion-doped TiO_2 thin films on mercury electrodeless discharge lamps: Preparation, characterization and their effect on the photocatalytic degradation of mono-chloroacetic acid and Rhodamine B. Journal of Chemical Technology and Biotechnology. 2009;**84**:1624-1630

[18] Wang JA, Limas-Ballesteros R, Lopez T. Quantitative determination of titanium lattice defects and solid-state reaction mechanism in iron-doped TiO_2 photocatalysts. Journal of Physical Chemistry B. 2001;**105**:9692-9698

[19] Laokiat L, Khemthong P, Grisdanurak N, Sreearunothai P, Pattanasiriwisawa W, Klysubun W. Photocatalytic degradation of benzene, toluene, ethylbenzene, and xylene (BTXE) using transition metal-doped titanium dioxide immobilized on fiberglass cloth. Korean Journal of Chemical Engineering. 2012;**29**:377-383

[20] Ambrus Z, Balazs N, Alapi T. Synthesis, structure and photocatalytic properties of Fe(III)-doped TiO_2 prepared from $TiCl_3$. Applied Catalysis B: Environmental. 2008;**81**:27-37

[21] Nagaveni K, Hedge MS, Madras G. Structure and photocatalytic activity of $Ti_{1-x}M_xO_{2\pm\delta}$ (M=W, V, Ce, Zr, Fe, and Cu) synthesized by solution combustion method. The Journal of Physical Chemistry B. 2004;**108**:20204-20212

[22] Japan Society of Mechanical Engineering. In: editors, editor. Heat Transfer Hand Book. 1st ed. Tokyo: Maruzen; 1993. p. 429

[23] Nishimura A, Mitsui G, Nakamura K, Hirota M, Hu E. CO_2 reforming characteristics under visible light response of Cr- or Ag-doped TiO_2 prepared by sol-gel and dip-coating process. International Journal of Photoenergy. 2012;**2012**:184169

[24] Goren Z, Willner I, Nelson AJ, Frank AJ. Selective photoreduction of CO_2/HCO_3^- to formate by aqueous suspensions and colloids of Pd-TiO_2. Journal of Physical Chemistry. 1990;**94**:3784-3790

[25] Tseng I-H, Chang W-C, Wu JCS. Photoreduction of CO_2 using sol-gel derived titania and titania-supported copper catalysts. Applied Catalysis B: Environmental. 2002;**37**:37-48

[26] Nishimura A, Sugiura N, Fujita M, Kato S, Kato S. Influence of preparation conditions of coated TiO_2 film on CO_2 reforming performance. Kagaku Kogaku Ronbunshu. 2007;**33**:146-153

[27] Nishimura A, Komatsu N, Mitsui G, Hirota M, Hu E. CO_2 reforming into fuel using TiO_2 photocatalyst and gas separation membrane. Catalysis Today. 2009;**148**:341-349

[28] Nishimura A, Okano Y, Hirota M, Hu E. Effect of preparation condition of TiO_2 film and experimental condition on CO_2 reduction performance of TiO_2 photocatalyst membrane reactor. International Journal of Photoenergy. 2011;**2011**:305650

[29] Marci G, Garcia-Lopez EI, Palmisano L. Photocatalytic CO_2 reduction in gas-solid regime in the presence of H_2O by using GaP/TiO_2 composite as photocatalyst under simulated solar light. Catalysis Communications. 2014;**53**:38-41

[30] Song G, Xin F, Yin X. Photocatalytic reduction of CO_2 in cyclohexanol on CdS-TiO_2 heterostructured photocatalyst. Applied analysis A: General. 2014;**473**:90-95

[31] Song G, Xin F, Yin X. Photocatalytic reduction of carbon dioxide over $ZnFe_2O_4$/TiO_2 nanobelts heterostructure in cyclohexanol. Journal of Colloid and Interface Science. 2015;**442**:60-66